Distortion in Quenching an AISI 4140 steel C-Ring-

Predictions and Experiments

da Silva, A. D.[a], Pedrosa, T. A.[b], Gonzalez-Mendez, J. L.[c], Xiaohui, J.[d], Cetlin, P. R.[e], and Altan, T.[f].

[a] *Research Engineer, College of Engineering, The Ohio State University, 339 Baker Systems/1972 Neil Avenue, Columbus, Ohio, 43210-1271, USA, and Graduate Student, School of Engineering, Federal University of Minas Gerais, Brazil (lissonds@gmail.com).*

[b] *Assistant Researcher, CNEN (Brazilian National Commission of Nuclear Energy), CDTN (Center for the Development of Nuclear Energy), Av. Antonio Carlos 6627, 31270-901, Belo Horizonte, Minas Gerais, Brazil (tap@cdtn.br).*

[c] *Graduate Student, College of Engineering, The Ohio State University, 339 Baker Systems/1972 Neil Avenue, Columbus, Ohio, 43210-1271, USA (gonzalez-mendez.1@buckeyemail.osu.edu).*

[d] *Research Engineer, College of Engineering, The Ohio State University, 339 Baker Systems/1972 Neil Avenue, Columbus, Ohio, 43210-1271, USA (11xiaoyuyu11@mail.dhu.edu.cn).*

[e] *Professor, Department of Mechanical Engineering, School of Engineering, Federal University of Minas Gerais, Av. Antonio Carlos 6627, 31270-901, Belo Horizonte, Minas Gerais, Brazil (pcetlin@demec.ufmg.br).*

[f] *Professor, College of Engineering, The Ohio State University, 339 Baker Systems/1972 Neil Avenue, Columbus, Ohio, 43210-1271, USA (altan.1@osu.edu).*

Abstract

Heat treatment processes are used to enhance the material properties of a wide range of mechanical steel components, according to their final application. Quenching is a common step in these heat treatments, involving the fast cooling of previously austenitized parts and leading to a phase transformation from austenite to hard martensite in the material. Quenching commonly causes a geometric distortion in the parts, associated with the thermal contraction and with the change in the mechanical and geometrical properties of austenite and martensite.

This study presents the results of a finite element (FE) simulation of the quenching of an AISI 4140 steel C-ring in oil, covering the analysis of the distortion caused by both thermal contraction and phase transformation. Furthermore, the distortion behavior during the cooling stage is analyzed, as well as the hardness and martensite volume fractions. Experiments were also conducted in order to obtain the geometric distortion, the microstructures and hardness of the C-rings. The FE modeling results are in good agreement with the experimental values.

Keywords: Distortion; quenching; heat treatment simulation; C-ring; 4140 steel; martensite; microstructure; hardness.

---

1. Introduction

Heat treatment is used to improve some of the mechanical properties of steel components, and commonly involves a quenching step which may cause undesired geometrical distortions in the processed parts. The dimensional accuracy of these parts is affected and leads to production and economical losses. An example of this situation is the production of rolled and heat treated rings with large diameters and small thickness, where quenching causes out-of-roundness of rings. It is frequently possible to minimize this distortion through the control of the heat transfer coefficient around the ring (Li et al., 2006), but a variety of ring sizes and materials quenched in the same production line make this approach not practical. As a result, distorted rings must undergo a radial compression or a radial expansion step, based on prior industrial experience, in order to correct the out-of-roundness shape, increasing production time and costs.

Arimoto et al. (2008) have performed a finite element simulation of the quenching of carburized 4140 steel rings (75 mm OD), discussing the origin of the quench distortion, considering carbon concentration, temperature evolution and volume fraction of the various metallic phases. The Navy C type test was described by Narazaki and Totten (2006) as a procedure to evaluate the

propensity for quench distortion in several materials. Fukuzumi and Yoshimura (1992) used this test to investigate the influence of the chemical composition on the hardenability and quench distortion for steels used in automobile steel gears. Cyril et al. (2009) have studied the distortion of C-rings and discussed the complexity of the numerical simulation of heat treatment distortions; their results were qualitatively, but not quantitatively, similar to the experimental ones. Brooks and Beckermann (2007) conducted numerical simulations and experimental tests for the quenching of cast steel C-rings, but did not obtain an adequate correlation for the experimental and predicted magnitudes of the distortions. Experimental quenching of C-ring specimens for different materials (including 4140 steel) have been conducted by Totten et al. (1993), who reported the resulting gap opening and outside diameter of the C-rings. Hardin and Beckermann (2005) simulated the quenching of C-rings based on 4140 steel material data and reported large differences between their results and those reported in the literature.

No satisfactory comparison between numerical simulations and experimental results on the distortion and microstructural and hardness distribution could be found in the literature for quenched 4140 C-rings. The objective of the present paper is to present such an analysis. In this study, a good agreement was found between the experimental and simulation results.

2. Methodology

2.1 Experimental Procedure

The material employed for the C-ring was an AISI 4140, with the nominal composition (certified by the supplier) of 0.40% C, 0.20% Si, 0.85% Mn, 0.95% Cr, 0.20% Mo. The geometry and dimensions of the C-ring are given in Figure 1.

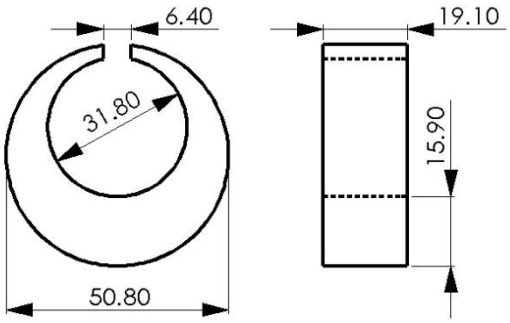

Figure 1 – C-ring geometry (all dimensions in mm).

The measurements of the ring dimensions before and after the heat treatment were performed in a Mitutoyo Shadowgraph PJ A3000 Model with an accuracy of 0.01 mm. Two dimensional changes were analyzed: gap opening, *G*, and outside diameter, *OD*. Based on Figure 2, the dimensional changes may be expressed as:

$$G = n' - n \ , \tag{1}$$

and,

$$OD = m' - m \ . \tag{2}$$

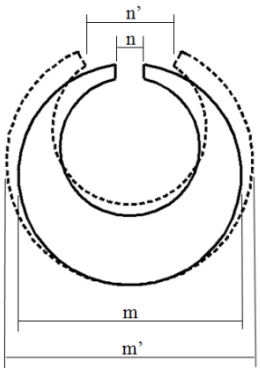

Figure 2 – C-ring specimen before heat treatment (*m* and *n* dimensions) and after heat treatment (*m'* and *n'* dimensions).

The rings were heated to 900 °C in a tubular furnace where an Argon gas flow was maintained for minimizing the oxidation of the material, and held at this temperature 3600 s in order to attain a homogeneous austenitic microstructure. Quenching was then performed through the

fast vertical movement of the ring (thickest part of the ring at the bottom and ring gap at the top) into the quenching oil (CASTROL ILOQUENCH 1) at 25 ºC, where it was held for at least 300 s.

The microstructure of the quenched C-rings was evaluated at various points of the longitudinal and transversal cross-sections of the C-rings, as illustrated in Figure 3. Sample preparation involved conventional surface grinding, polishing and etching with Nital 2%. Hardness measurements (HRC – Rockwell “C”) were taken at various locations in the sections indicated in Figure 3.

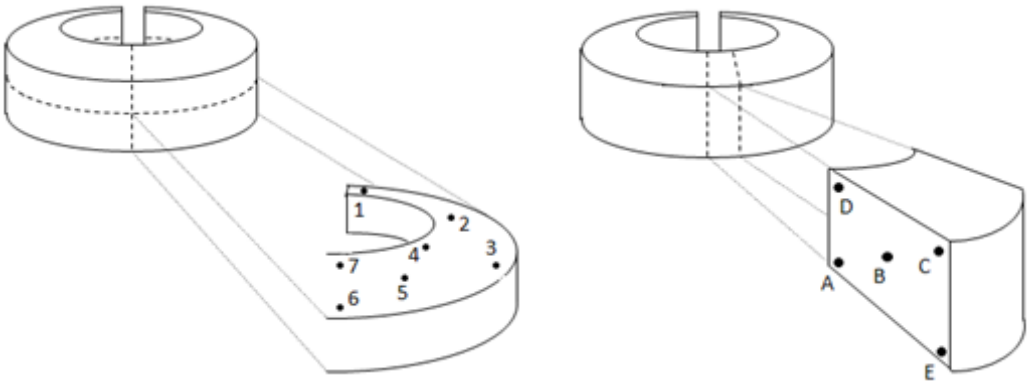

(a) (b)

Figure 3 – Location of the regions where the microstructure of the quenched C-rings was examined (a) in the longitudinal cross-section and (b) in the transversal cross-section.

2.2 Numerical Simulation

The present simulations utilized the software DEFORM^{TM}-HT module, version 10.1 (Scientific Forming Technology Corporation, Columbus, Ohio, USA), based on the Finite Element Method, establishing a coupling between all of the involved phenomena as shown in Figure 4. The part distortion was predicted taking into account the deformation based on the following strain rate components:

$$\dot{\varepsilon}_{ij} = \dot{\varepsilon}_{ij}^{e} + \dot{\varepsilon}_{ij}^{p} + \dot{\varepsilon}_{ij}^{th} + \dot{\varepsilon}_{ij}^{tr} + \dot{\varepsilon}_{ij}^{tp} \quad (3)$$

where *e*, *p*, *th*, *tr*, and *tp* represent the contributions from elastic, plastic, thermal, phase transformation and transformation plasticity, respectively.

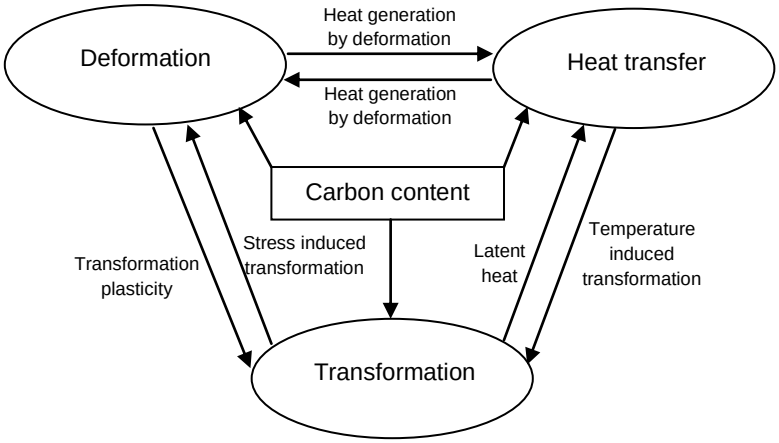

Figure 4 - Coupled phenomena considered during the quenching simulations.

In order to obtain adequate simulation results the material data should be accurate. According to Guo et al. (2009) the following information on materials properties have to be known for distortion prediction caused by quenching through numerical simulations:

- phase transformation kinetics, *i.e.*, TTT and CCT diagrams;
- temperature dependent thermo-physical properties for each phase formed, such as density, Young's modulus, thermal expansion coefficient, and thermal conductivity;
- temperature dependent mechanical properties of each phase formed, including tensile strength, yield strength, and hardness.

The above data involves long and expensive laboratory testing; an alternative is the use of softwares focused on material properties simulation, which are usually based on the chemical composition of the material. The present simulation of the C-ring quenching utilized data in the material library of DEFORM^{TM} and the material properties for the 4140 steel provided by JMatPro (Sente Software Ltd., Surrey, United Kingdom).

The simulation of the initial heating stage of the C-ring involved the prediction of the ring expansion due to the temperature increase from 20 to 900 °C. The coefficient of thermal expansion as a function of temperature for the 4140 steel was obtained from the DEFORM^{TM}

library. Once expanded at 900 °C, the specimen was considered as completely austenitized (100% austenite).

The AISI 4140 data for the quenching stage simulation was obtained from the JMatPro software. The mechanical and thermo-physical properties for the various material phases and constituents (austenite, martensite, bainite, ferrite and pearlite) are taken into consideration. The phase transformation kinetics are based on TTT curves. All of the transformation aspects are taken into account, including latent heat, volume change and transformation plasticity. Jominy curves are used for hardness prediction.

Xiao et al. (2010) have shown that the quench orientation and bath agitation conditions influence the heat transfer between the part and the quenchant; the heat transfer may also vary along the various part surfaces. Since that the C-ring has a relatively small size and the quenching process was performed in still oil, the heat transfer coefficient was considered constant along all of the C-ring surface and as a function only of the ring surface temperature. Hardin and Beckermann (2005) determined the heat transfer coefficient between AISI 4140 and oil as a function of temperature, which was used in the present simulation. Figure 5 shows the heat transfer coefficient in function of surface temperature.

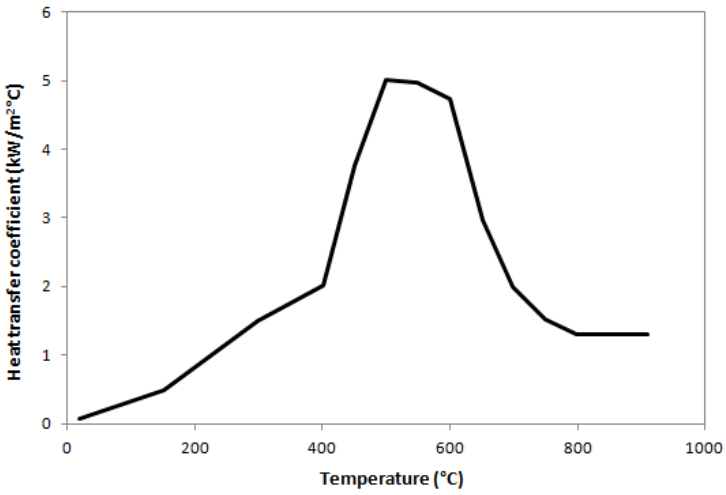

Figure 5 – Heat transfer coefficient between AISI 4140 and still oil (Hardin and Beckermann, 2005).

Due to the part symmetry, only ¼ of the part was simulated. Brick elements were used (7,000), as shown in Figure 6. Nodes *M* and *N* were utilized for outside diameter and gap opening measurements, respectively. Table 1 summarizes the FE setup for the simulations.

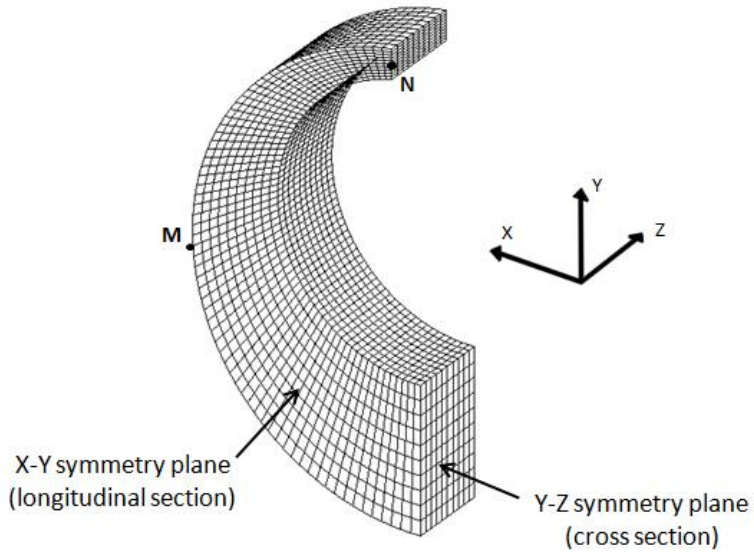

Figure 6 – Meshed ¼ symmetric geometry, used for the simulation. Nodes *M* and *N* were used for outside diameter and gap opening evaluation, respectively.

Table 1 – FE setup for the simulations.

Operation	Parameter	Value
1 – Heating (furnace)	Code	DEFORM-3D™
	C-ring geometry	Figure 1
	Material	AISI 4140 from DEFORM-3D™ library
	Initial temperature	20 °C
	Furnace temperature	900 °C
	Object type	Elastic
2 – Quenching (oil)	Code	DEFORM-3D™
	C-ring geometry	Expanded - Operation 1
	Material	AISI 4140 from JMatPro
	Initial temperature	900 °C
	Quenchant temperature	25 °C
	Heat transfer coefficient	Function of temperature (Figure 5)
	Object type	Elasto-plastic

3. Results and Discussion

3.1. Distortion of the C-rings

Figure 7 shows the simulated distribution of the displacement in the *x* direction for the points in the longitudinal cross-section of the C-ring. There is a tendency for the “opening” of the ring, as observed experimentally. Figure 8 displays the simulated displacements in the *x* direction of nodes *N* and *M* in the C-ring for a period of 150 s after the beginning of the quenching process. It is seen that after about 100 s, there is a stabilization of the displacements predicted for both nodes. Taking into account that a symmetric FE model has been used, the x-displacement, given in Figure 8, represents only half of the total displacement. Thus, the ring gap opens 0.402 mm and the outer diameter expands about 0.084 mm. Table 2 presents a comparison between the experimental and predicted values for the ring distortion. It is seen that the relative difference for gap opening and outside diameter increase are smaller than 7%.

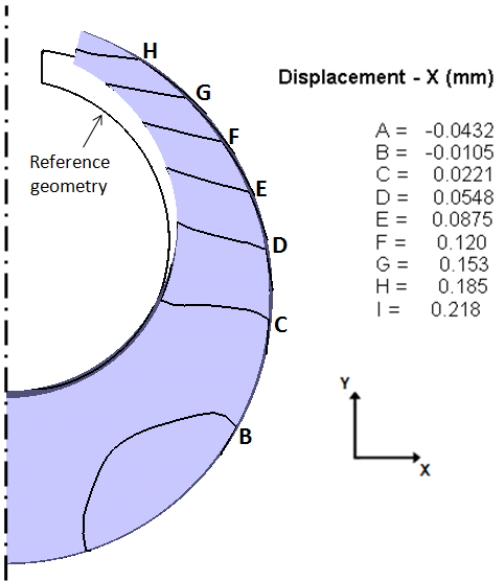

Figure 7 – Simulated displacement in the *x* direction of the points in the longitudinal cross-section of the C-ring (displaced geometry magnified 20x).

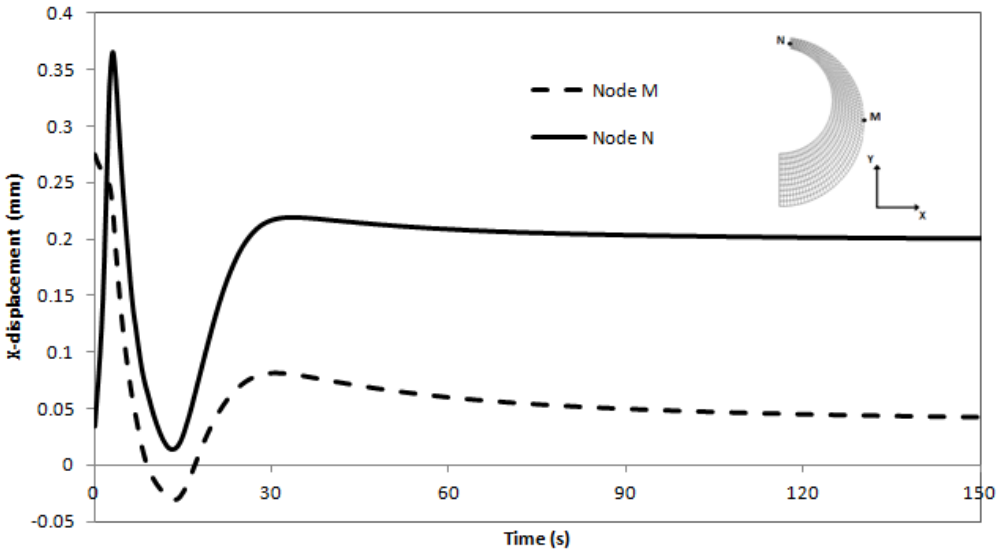

Figure 8 – Simulated displacements in the *x* direction for Nodes *N* and *M* of the C-ring, during the oil quenching process.

Table 2 – Comparison of the experimental and simulated results for the geometrical distortions of the C-ring.

Dimensional changes	Method		Prediction difference (%)
	Experimental	Simulation	
Gap opening (mm)	0.43	0.402	6.5%
Outside diameter (mm)	0.09	0.084	6.7%

3.2 Microstructures and hardness

Table 3 displays the values of hardness measured at the various locations in the cross-sections of the C-rings indicated in Figure 3. All values lie between 54 and 55 HRC, confirming the formation of high fractions of martensite (Gür and Tuncer, 2004). This is fully confirmed by the various metallographic results given in Figures 9 and 10.

Table 2 – Measured hardness after oil quenching process.

Property	C-ring region											
	A	B	C	D	E	1	2	3	4	5	6	7
Hardness (HRC)	54	54	54	55	55	54	55	54	54	55	54	54

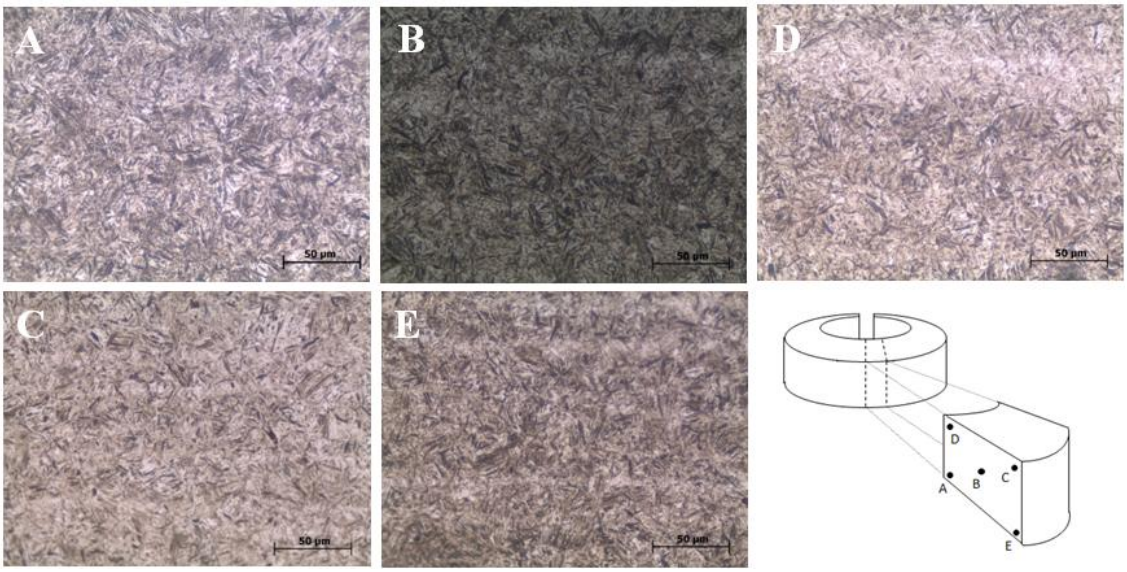

Figure 9 – Micrographs from various points in the transversal cross-section of a C-ring, indicating the presence of martensite in all locations (optical microscopy).

Figure 11 shows the simulated distribution of martensite on the C-ring surface and of the displacement. The specimen was initially thermally expanded and austenitized. From 4 s after the quench initiation, it is possible to visualize in Figure 11 the beginning of martensite formation in the region close to the C-ring gap. After 10 s, practically all thermal expansion is absent, but martensite formation is still in progress, being now responsible for further ring distortions. The situation after 25 s of cooling shows that the martensite formation in the thicker portion of the C-ring is associated with the final opening of the ring gap and of the external diameter of the ring.

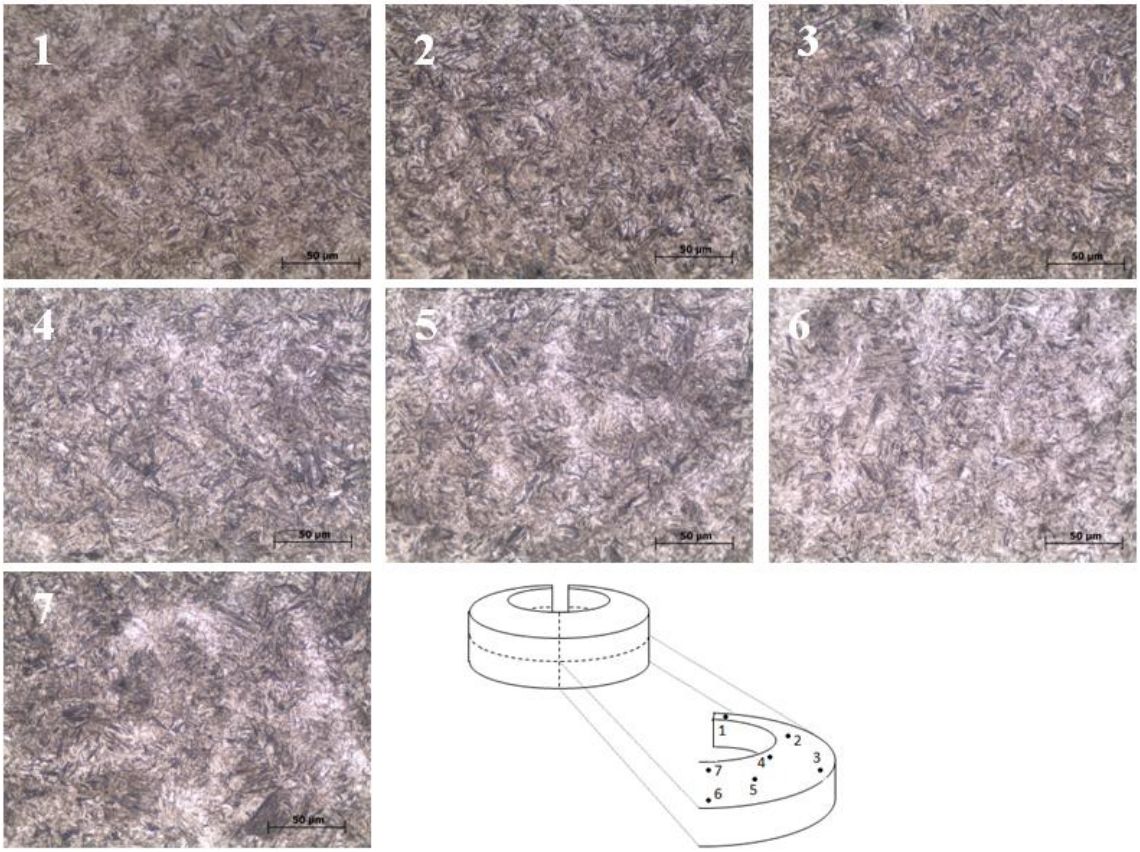

Figure 10 – Micrographs from various points in the longitudinal cross-section of a C-ring, indicating the presence of martensite in all locations (optical microscopy).

Figures 12 and 13 display the simulated results for the evolution of martensite volume fraction for various points in the transversal and longitudinal cross-sections of the C-ring, respectively. Very high volume fraction of martensite are predicted, in agreement with the metallographic and hardness results displayed in Table 3 and Figures 9 and 10. The simulated hardness values lie around 56 HRC, again in agreement with the experimentally measured values.

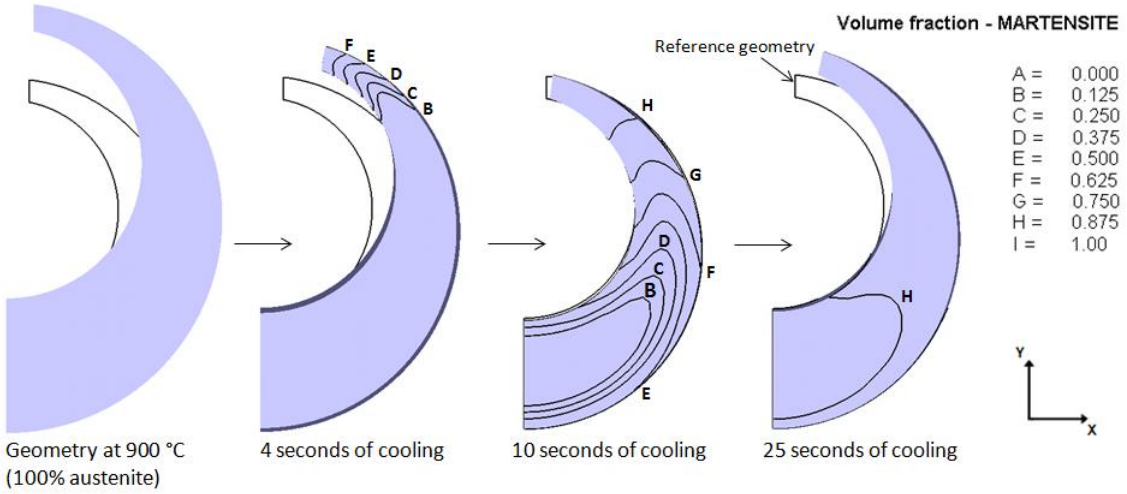

Figure 11 – Martensite formation (displaced geometry magnified 20x) on the C-ring during the cooling simulation.

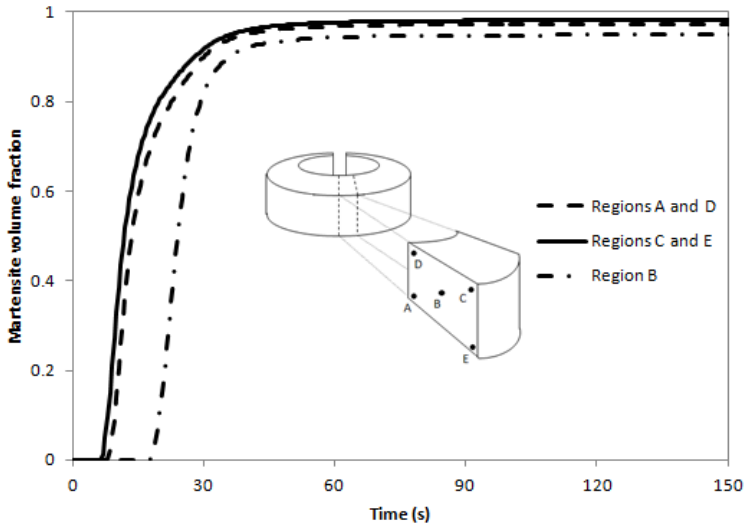

Figure 12 – Simulated evolution of the martensite volume fraction at several points in the transversal cross-section of the C-ring during oil quenching.

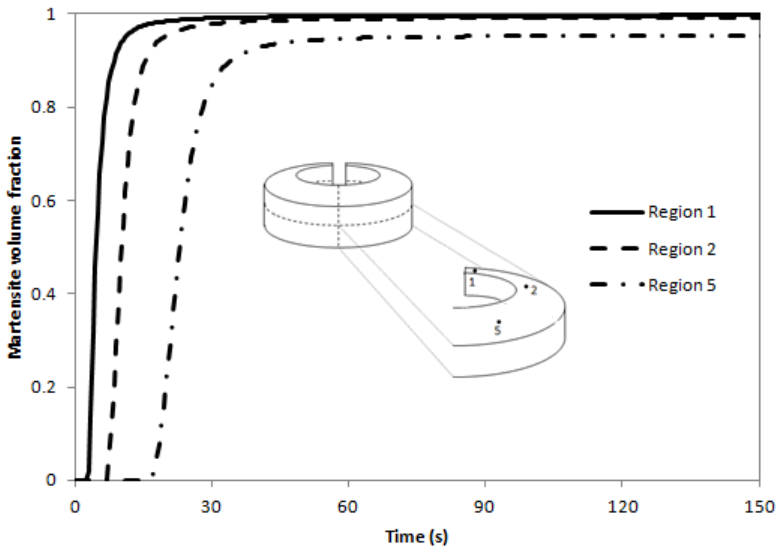

Figure 13 – Simulated evolution of the martensite volume fraction at several points in the longitudinal cross-section of the C-ring during oil quenching.

4. Conclusions

The experimental quenching of the AISI 4140 steel C-rings (Figure 1) in oil leads to an increase in both ring gap and outside diameter, as well as to a fully martensitic microstructure at all points of C-ring, with a hardness of about 55 HRC.

The simulation of quenching, using the DEFORM^{TM} software and thermo-physical material data from JMatPro, led to results very similar to those obtained experimentally, for both geometric distortions and final microstructures and hardness. The maximum difference between the experimental and the simulated values for the C-ring gap opening and the increase in ring diameter was about 7%; final hardness prediction was 56 HRC.

According to the simulation, the geometric distortion of the C-ring is associated with the austenite to martensite transformation at the thickest part of the ring, during the final stages of the quenching process.

Acknowledgements

The authors of this work would like to thank:

- CNPq (Brazilian National Research and Development Council), for the “sandwich” Ph.D. scholarship (SWE) and financial support to the project;
- FAPEMIG (Foundation for the Support of Research in the Minas Gerais State), for the financial support to the project;
- SFTC (Scientific Forming Technologies, USA), for the assistance during heat treatment distortion simulation development;
- Sente Software Ltd., UK for providing AISI 4140 material data, based on JMatPro, for the simulation;
- and Dr. George Totten, for the assistance with the Navy C-Ring test.

References

Arimoto, K., Yamanaka, S., & Funatani, K., 2008. Explanation of the Origin of Distortion and Residual Stress in Carburized Ring Using Computer Simulation. Journal of ASTM International. 5, 1-9.

Brooks, B.E., and Beckermann, C., 2007. Prediction of Heat Treatment Distortion of Cast Steel C-Rings. Proceedings of the 61st SFSA Technical and Operating Conference, Chicago, USA, 4.5, 1-30.

Cyril, N., Cyrille, B., Stéphane, L., Mihaela, T., & Régis, B., 2009. Comparison of experimental and simulation distortions of quenched C-ring test parts. International Journal of Material Forming. 2, 263-266.

Fukuzumi, T., & Yoshimura, T., 1992. Reduction of distortion caused by heat treatment on automobile steel gear. Proceedings of the First International Conference on Quenching & Control of Distortion, Chicago, USA, 199-203.

Guo, Z., Saunders, N., Miodownik, P., & Schillé, J.-P., 2009. Modelling phase transformations and material properties critical to the prediction of distortion during the heat treatment of steels. International Journal of Microstructure and Materials Properties. 4, 187-195.

Gür, C. H., & Tuncer, B. O., 2004. Investigating the Microstructure-Ultrasonic Property Relationships in Steels. 16th World Conference on Nondestructive testing, Montreal, Canada, 1-7.

Hardin, R. A., & Beckermann, C., 2005. Simulation of Heat Treatment Distortion. Proceedings of the 59th SFSA Technical and Operating Conference, 3.3, 1-3.

Li, Z., Grandhi, R. V., & Srinivasan, R., 2006. Distortion minimization during gas quenching process. Journal of Materials Processing Technology. 178, 249-257.

Totten, G. E., Bates, C. E., & Clinton, N. A., 1993. Handbook of Quenchants and Quenching, ASM International, Materials Park, pp. 485-492.

Xiao, B., Wang, Q., Jadhav, P., & Li, K., 2010. An Experimental Study of Heat Transfer in Aluminum Castings During Water Quenching. Journal of Materials Processing Technology. 210, 2023-2028.

Figure 1

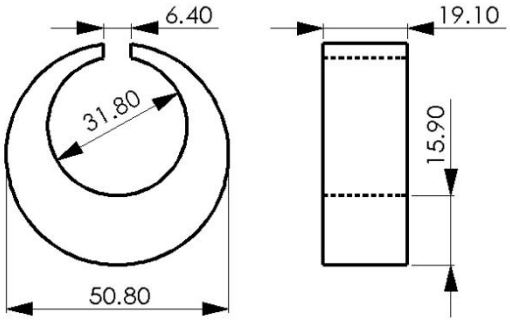

Figure 2

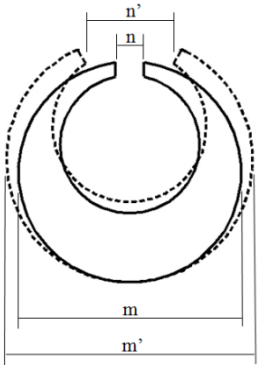

Figure 3

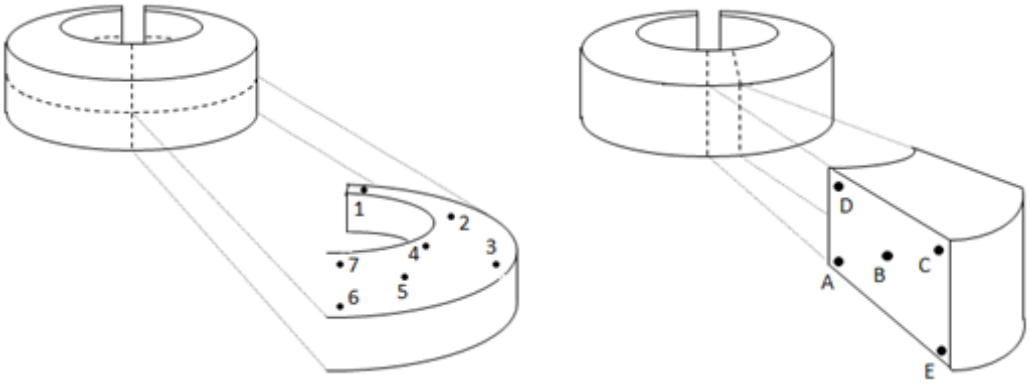

(a) (b)

Figure 4

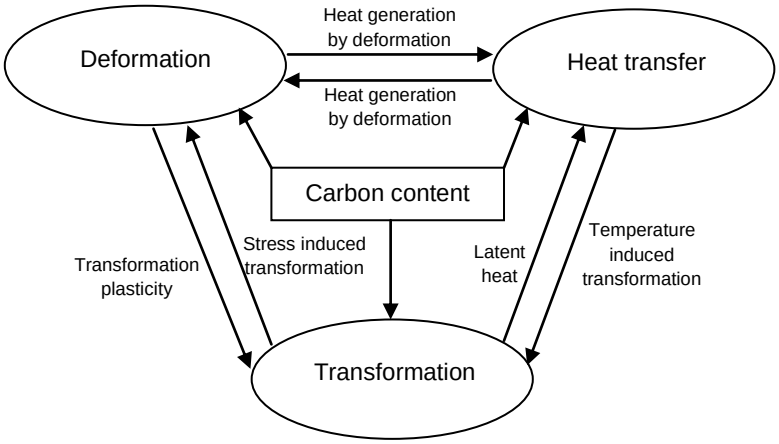
Deformation
Heat generation
by deformation
Heat transfer
Heat generation
by deformation
Carbon content
Transformation
plasticity
Stress induced
transformation
Latent
heat
Temperature
induced
transformation
Transformation

Figure 5

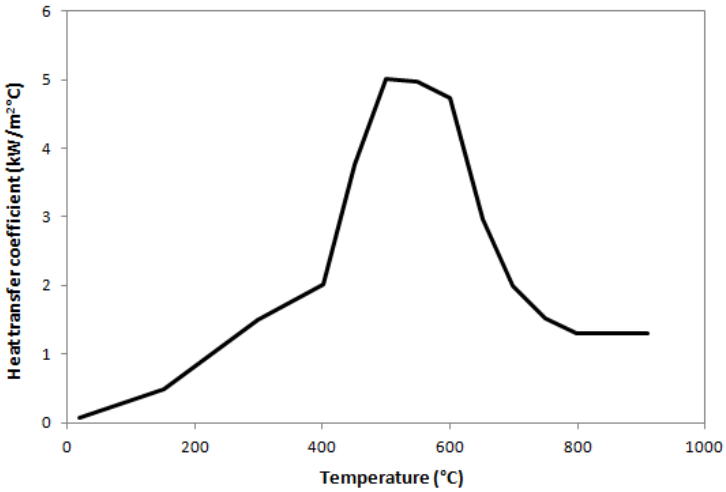
Heat transfer coefficient (kW/m²°C)
0
1
2
3
4
5
6
0
200
400
600
800
1000
Temperature (°C)

Figure 6

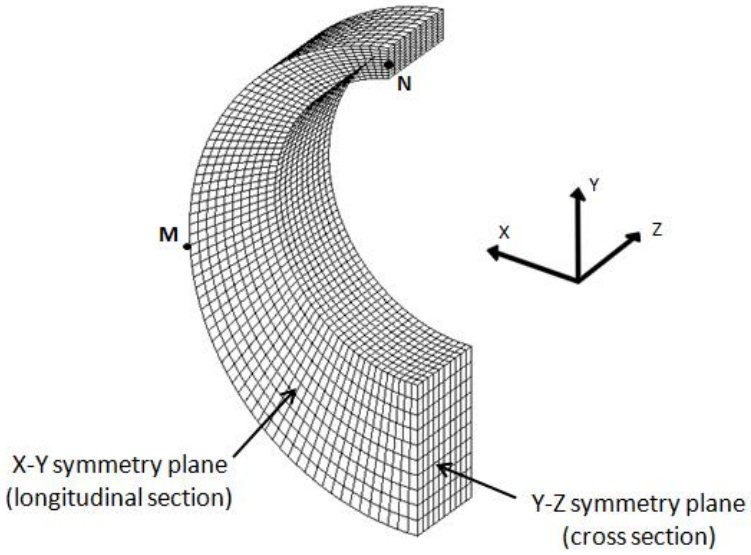
N
M
Y
X
Z
X-Y symmetry plane
(longitudinal section)
Y-Z symmetry plane
(cross section)

Figure 7

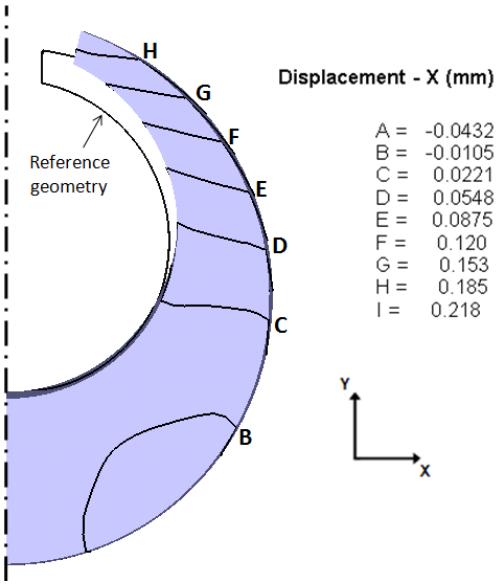
H
G
F
E
D
C
B
Reference geometry
Displacement - X (mm)
A = -0.0432
B = -0.0105
C = 0.0221
D = 0.0548
E = 0.0875
F = 0.120
G = 0.153
H = 0.185
I = 0.218
Y
X

Figure 8

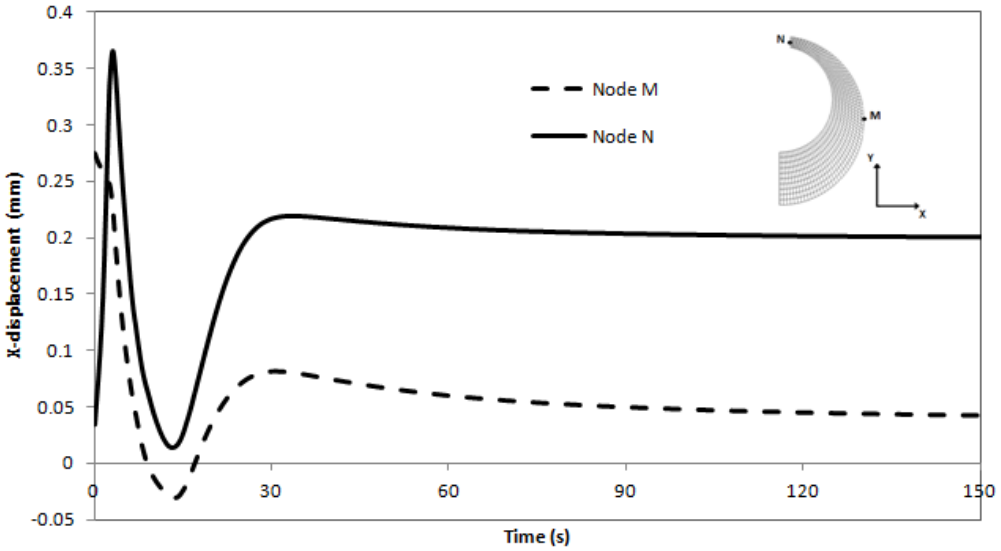
0.4
0.35
0.3
0.25
0.2
0.15
0.1
0.05
0
-0.05
X-displacement (mm)
0
30
60
90
120
150
Time (s)
Node M
Node N
N
M
Y
X

Figure 9

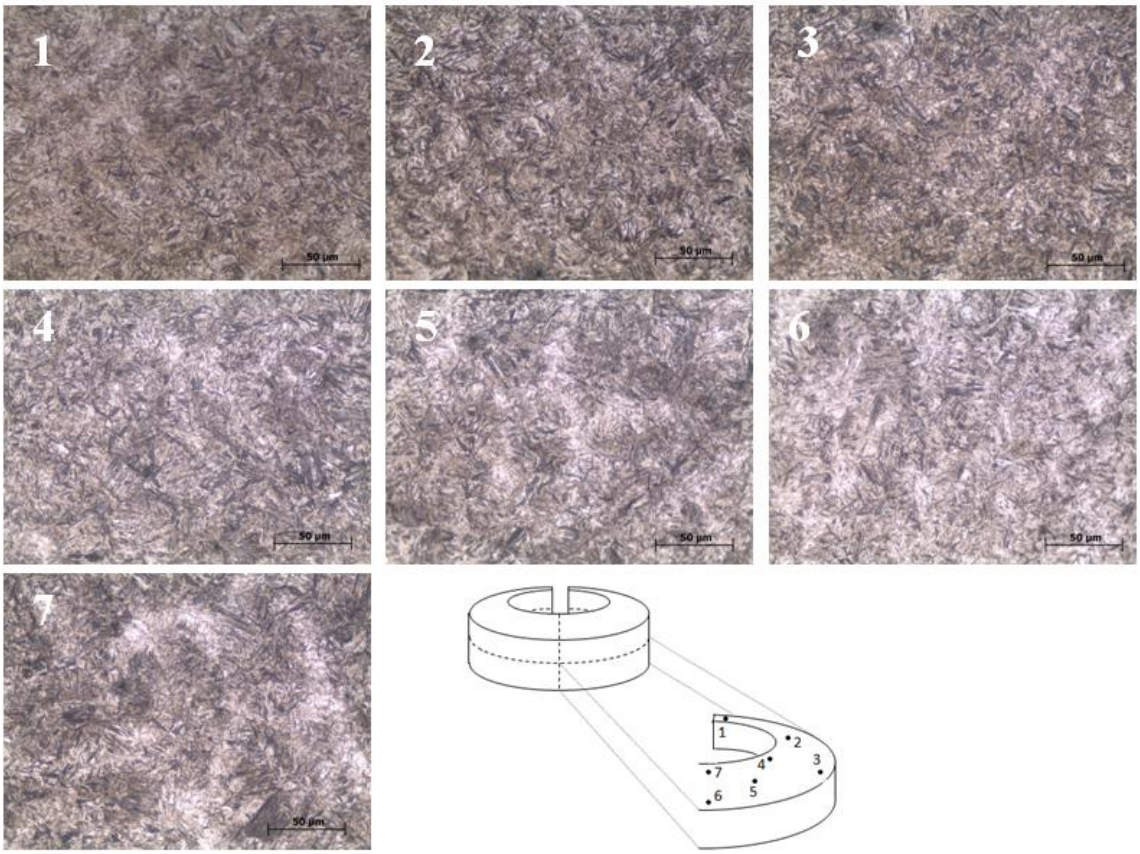

Figure 10

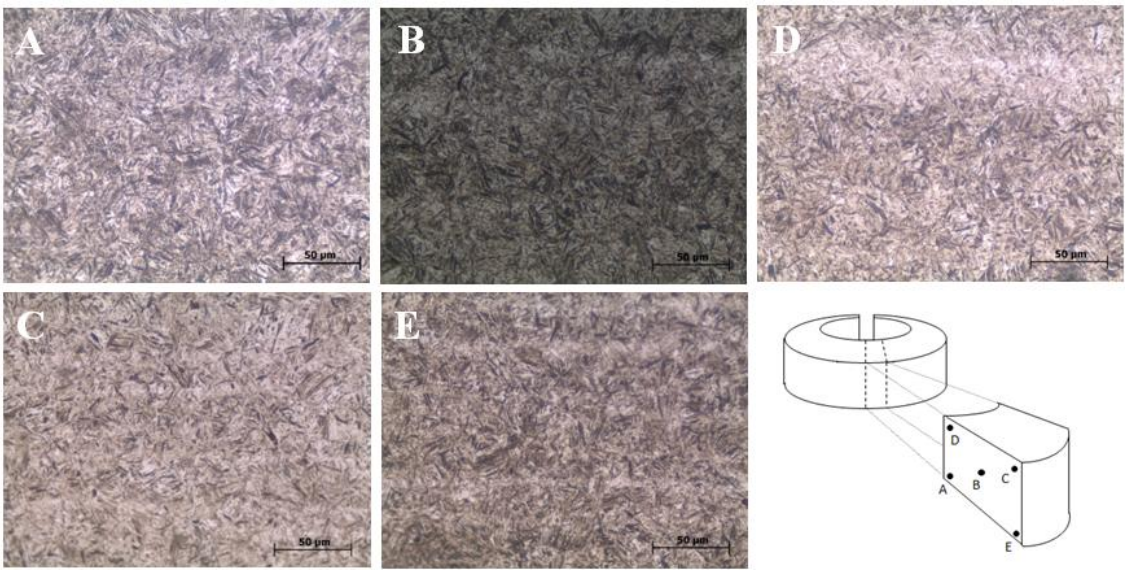

Figure 11

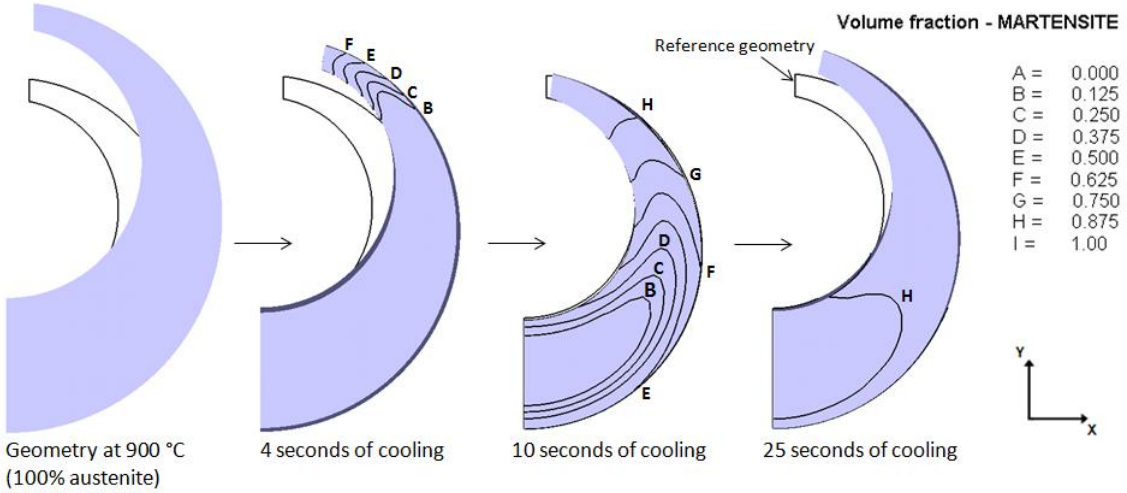
Volume fraction - MARTENSITE
Reference geometry
A = 0.000
B = 0.125
C = 0.250
D = 0.375
E = 0.500
F = 0.625
G = 0.750
H = 0.875
I = 1.00
Y
X
Geometry at 900 °C
(100% austenite)
4 seconds of cooling
10 seconds of cooling
25 seconds of cooling

Figure 12

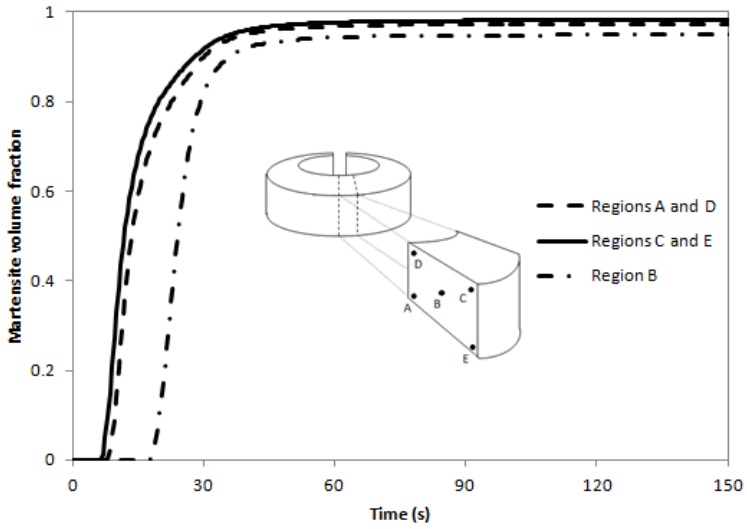
Martensite volume fraction
1
0.8
0.6
0.4
0.2
0
0
30
60
90
120
150
Time (s)
Regions A and D
Regions C and E
Region B
A
B
C
D
E

Figure 13

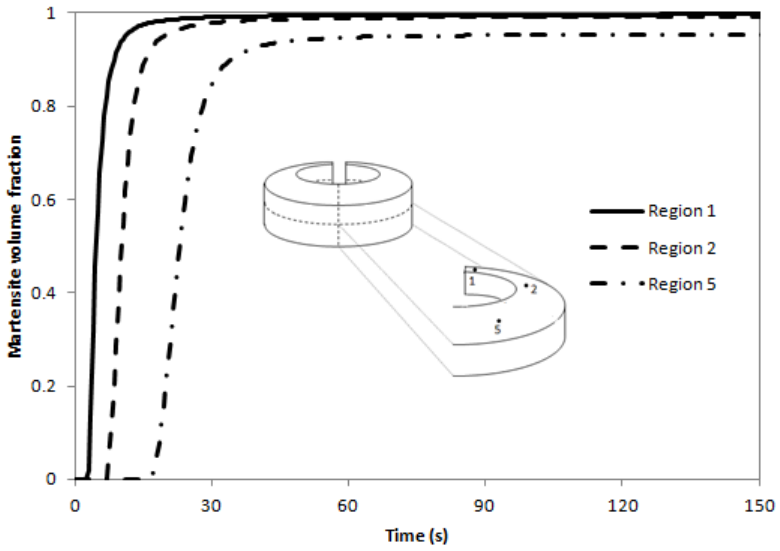
Martensite volume fraction
Time (s)
0
0.2
0.4
0.6
0.8
1
0
30
60
90
120
150
Region 1
Region 2
Region 5
1
2
5

Table 1

Operation	Parameter	Value
1 – Heating (furnace)	Code	DEFORM-3D™
	C-ring geometry	Figure 1
	Material	AISI 4140 from DEFORM-3D™ library
	Initial temperature	20 °C
	Furnace temperature	900 °C
	Object type	Elastic
2 – Quenching (oil)	Code	DEFORM-3D™
	C-ring geometry	Expanded - Operation 1
	Material	AISI 4140 from JMatPro
	Initial temperature	900 °C
	Quenchant temperature	25 °C
	Heat transfer coefficient	Function of temperature (Figure 5)
	Object type	Elasto-plastic

Table 2

Dimensional changes	Method		Prediction difference (%)
	Experimental	Simulation	
Gap opening (mm)	0.43	0.402	6.5%
Outside diameter (mm)	0.09	0.084	6.7%

Table 3

Property	C-ring region											
	A	B	C	D	E	1	2	3	4	5	6	7
Hardness (HRC)	54	54	54	55	55	54	55	54	54	55	54	54